

LETTER OPEN



ACUTE LYMPHOBLASTIC LEUKEMIA

How T-lymphoblastic leukemia can be classified based on genetics using standard diagnostic techniques enhanced by whole genome sequencing

Janine Müller¹, Wencke Walter ¹, Claudia Haferlach ¹, Heiko Müller¹, Irene Fuhrmann¹, Martha-Lena Müller¹, Henning Ruge¹, Manja Meggendorfer¹, Wolfgang Kern ¹, Torsten Haferlach ¹ and Anna Stengel ¹✉

© The Author(s) 2022, corrected publication 2022

Leukemia (2023) 37:217–221; <https://doi.org/10.1038/s41375-022-01743-6>

TO THE EDITOR:

With the introduction of the 5th edition of the WHO classification, the number of genetically defined entities in myeloid neoplasms and BCP-ALL has increased considerably [1, 2]. However, no genetically defined entity has been introduced in T-lymphoblastic leukemia (T-ALL), as genetic group assignment remains complex and the reproducibility between studies varies. In the International Consensus Classification (ICC) eight subgroups (*HOXA*-dysregulated-, *SPI1*-, *TLX1*-, *TLX3*-, *NKX2*-, *TAL1*-2-, *LMO1*-2-rearranged T-ALLs and T-ALLs with rearrangements with other helix-loop-helix family members like *LYL1* or *OLIG2/BHLHB1*) have been proposed as provisional entities, due to lack of consensus how to define different subtypes [3]. However, for a first step towards personalized medicine a distinct classification based on biomarkers assessable by routine diagnostic methods is essential. Thus, we analyzed 131 T-ALL sent to MLL Munich Leukemia Laboratory between 05/2008 and 12/2020 by chromosome banding analysis (CBA) ± fluorescence in situ hybridization (FISH) on interphase nuclei. Additionally, WGS (100×, 2 × 151bp) and WTS (50 Mio reads, 2 × 101 bp) were performed on a NovaSeq(ILMN). Variants were called with Strelka2, Manta and GATK using a tumor w/o normal pipeline, fusions with Arriba, STAR-Fusion and Manta. T-cell receptor (TCR) rearrangement analysis was based on WTS data (Supplementary material and Supplementary Table 1). All patients had given written informed consent to the use of genetic and clinical data according to the Declaration of Helsinki. The study was approved by the internal institutional review board of MLL.

Based on results of CBA supplemented by FISH with probes for detection of rearrangements involving *TRAD*, *TRB*, *TLX1*, *TLX3*, *NUP98*, and *HOXA9/10* and RT-PCR for detection of *STIL::TAL1*, *SET::NUP214* and *PICALM::MLLT10* 131 T-ALL cases were assigned to the following nine genetically defined subgroups: *TLX1*: structural alterations involving *TLX1*: $n = 22$; *TLX3*: structural alterations involving *TLX3*: $n = 10$, *TAL1*: structural alterations involving *TAL1*: $n = 3$, *HOXA9/10*: structural alterations involving *HOXA9/10* genes: $n = 4$, *SET::NUP214*: *SET::NUP214* fusion: $n = 7$, *MLLT10*: fusions involving *MLLT10*: $n = 4$, *NUP98*: fusions involving *NUP98*: $n = 3$, *MYB*: structural alterations involving *MYB*: $n = 2$, rare fusions

(*LEF1*-, *LMO2*- and *NKX2-3*-rearrangements): $n = 4$, and NOS: not otherwise specified - lacking all of the subgroup-defining alterations of groups 1–9: $n = 71$ (Fig. 1A, B).

The detection of abnormal T-ALL clones by CBA is hampered by reduced in vitro proliferation of leukemia cells leading to an insufficient number of metaphases or only metaphases with a normal karyotype from normal hematopoietic cells. Supplementary FISH or RT-PCR analyses were required for genetic subtype classification in 26/131 (20%) cases: 20 due to the cytogenetically cryptic nature of the abnormality and 6 due to insufficient in vitro proliferation of the T-ALL clone. Thus, in cases where no abnormalities have been detected, additional FISH screening should be performed. Furthermore, several abnormalities are not detectable by CBA due to its low resolution such as rearrangements of *BCL11B::TLX3*, *SET::NUP214* and *STIL::TAL1*. Therefore, for a comprehensive classification of T-ALL it is necessary to supplement CBA by FISH and RT-PCR.

Next, we evaluated whether WGS data can add relevant information for classification. Of note, all CBA ± FISH ± RT-PCR assignments were confirmed by WGS. In 13 cases, in which either no material for FISH was available ($n = 4$) or no FISH probes or RT-PCR were available for the detection of the respective abnormality ($n = 9$, *CCDC26::TLX3*, *DDX3X::MLLT10*, *XPO1::MLLT10*, *TRB::MYB*, *TRB::NOTCH1*; *MYB* enhancer mutation), WGS identified specific rearrangements (*TLX1*: 1; *TLX3*: 2, *HOXA9/10*: 2, *MLLT10*: 3, *MYB*: 2, rare rearrangements: 3 (*TRB::NOTCH1* ($n = 1$); *MYB* enhancer mutation ($n = 2$)). Further, 10 cases were assigned to the recently described *BCL11B*-rearranged subset (*CCDC26::BCL11B* ($n = 2$), *ARID1B::BCL11B* ($n = 2$), *SATB1::BCL11B* ($n = 1$), or *BCL11B* enhancer amplification ($n = 5$)) [4, 5]. Based on WGS data 83/131 cases (63%) were assigned to a specific genetic subgroup and only 37% of cases were labeled “not otherwise specified”. *BCL11B* rearrangements are found in T-ALL, MPAL and immature AML [4, 5], advocating the introduction of *BCL11B* FISH probes into routine diagnostics for classification of acute leukemia’s of ambiguous lineage according to the 5th edition of the WHO classification [1].

A comprehensive clinical and genetic workup revealed that the subtypes showed distinct characteristics (Fig. 2). The *TLX1*- and

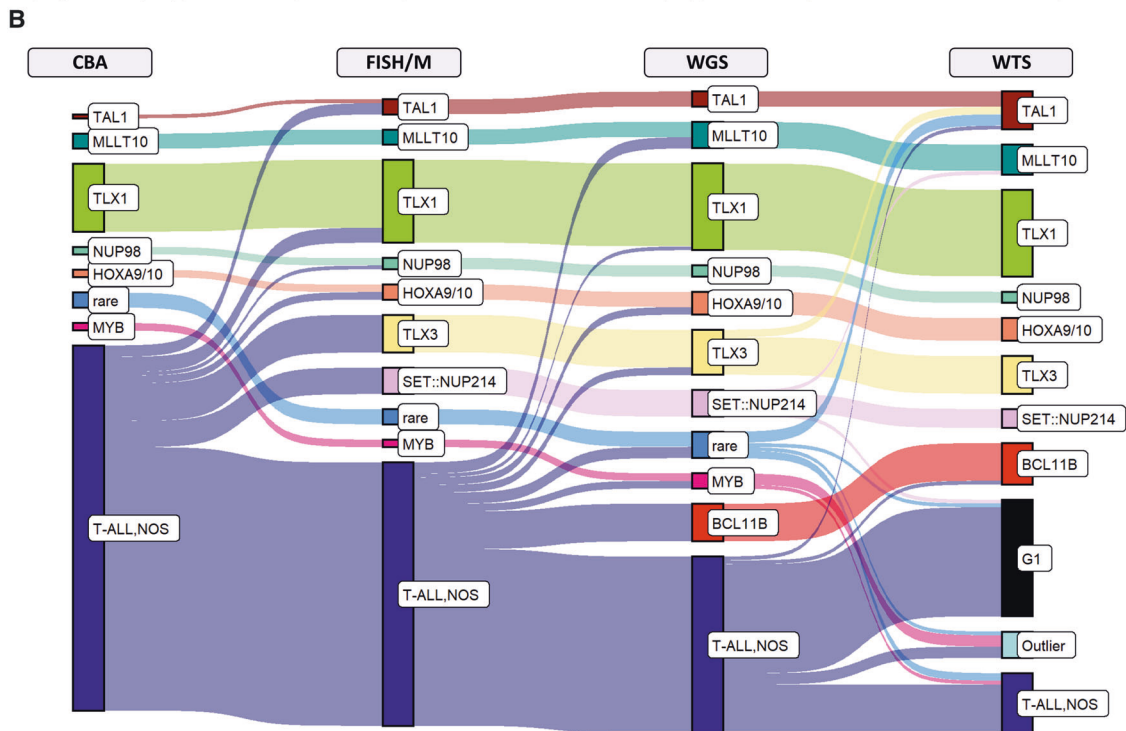
¹MLL Munich Leukemia Laboratory, Max-Lebsche-Platz 31, 81377 Munich, Germany. ✉email: anna.stengel@mll.com

Received: 19 August 2022 Revised: 18 October 2022 Accepted: 20 October 2022
Published online: 5 November 2022

A Genetic classification of 131 T-ALL samples

Genetic subgroup	Primary aberrations	FISH probes	Fusion genes	Standard diagnostic			
				CBA	FISH	M	WGS
TLX1	t(10;14)(q24;q11); <i>TRAD::TLX1</i>	<i>TLX1 BA</i>	—	■	■	■	■
	t(7;10)(q34;q24); <i>TRB::TLX1</i>	<i>TLX1 BA</i>	—	■	■	■	■
TLX3	t(5;14)(q35;q32)*; <i>BCL11B::TLX3</i>	<i>BCL11B::TLX3, TLX3 BA</i>	—	■	■	■	■
TAL1	t(1;14)(p32;q11); <i>TRAD::TAL1</i>	<i>TRAD BA**</i>	—	■	■	■	■
	del(1)(p32p32)*	—	<i>STIL::TAL1</i>	■	■	■	■
HOXA9/10	inv(7)(p15q34); <i>HOXA::TRB</i>	<i>HOXA BA</i>	—	■	■	■	■
SET::NUP214	del(9)(q34q34)*	—	<i>SET::NUP214</i>	■	■	■	■
MLLT10	t(10;11)(p12;q14)	—	<i>PICALM::MLLT10</i>	■	■	■	■
	t(X;10)(p11;p12)	—	<i>DDX3X::MLLT10</i>	■	■	■	■
NUP98	t(4;11)(q23;p15)	<i>NUP98 BA</i>	<i>NUP98::RAP1GDS1</i>	■	■	■	■
MYB	t(6;7)(q23;q34); <i>TRB::MYB</i>	<i>TRAD BA**</i>	—	■	■	■	■
BCL11B	t(8;14)(q24;q32); <i>BCL11B::CCDC26*</i>	—	—	■	■	■	■
	t(6;14)(q25;q32); <i>BCL11B::ARID1B*</i>	—	—	■	■	■	■
	t(3;14)(p24;q32); <i>BCL11B::SATB1</i>	—	—	■	■	■	■
	BCL11B enhancer amplification	—	—	■	■	■	■
rare	t(4;14)(q25;q11); <i>TRAD::LEF1</i>	<i>TRAD BA**</i>	—	■	■	■	■
	t(11;14)(p13;q11); <i>TRAD::LMO2</i>	<i>TRAD BA**</i>	—	■	■	■	■
	t(7;10)(q34;q24); <i>TRB::NKX2</i>	<i>TRB BA**</i>	—	■	■	■	■
	t(7;9)(q34;q34); <i>TRB::NOTCH1</i>	<i>TRB BA**</i>	—	■	■	■	■
	t(11;14)(p13;q32); <i>LMO2</i>	—	—	■	■	■	■
Mutation in MYB enhancer	—	—	■	■	■	■	

* cytogenetically cryptic **if interphase-FISH positive in ALL with normal karyotype, searching with FISH for aberrant metaphases



TLX3 group were associated with young age (median age: 37 years, range 20–60 years; 22 years, 5–75 years), a strong male preponderance (male: female 6.7:1; 3:1), as well as a high rate of *CDKN2A* deletions (22/23, 96%; 10/12, 83%), a high frequency of *NOTCH1* (21/23, 91%; 11/12, 92%) and *PHF6* mutations (12/23, 52%;

7/12, 58%). A high frequency of *WT1* mutations was found in the TLX3-group (5/12; 41.7%).

Patients assigned to the groups TAL1, HOXA9/10, SET::NUP214, MLLT10-fusions, and NUP98-fusions were also younger compared to the BCL11B- and NOS group (median

Fig. 1 Definition and detection of T-ALL subtypes. **A** In conjunction with cytogenetics, molecular genetics and WGS, the cohort was classified into 9 distinct subtypes based on their primary genetic event. While translocations can be detected with CBA or commercially available FISH probes, gene fusions are detected by molecular genetics. The drawing on the right shows which method is suitable for detecting the respective alteration; green: detectable, yellow: the translocation is only detectable in conjunction with CBA, in which fluorescence in situ hybridization on metaphases identifies the partner chromosome of 14q11 (TRAD) or 7q34 (TRB); yellow shaded: basically detectable; however, commercially available FISH probes are lacking for translocations; for rare fusions a PCR has to be established, red: not detectable; CBA: chromosome banding analysis; FISH: fluorescence in situ hybridization, M: molecular genetics; WGS: whole genome sequencing. **B** The Sankey diagram shows the shift in classification depending on the method applied. The height of the bars represents the relative distribution of the genetic subgroups.

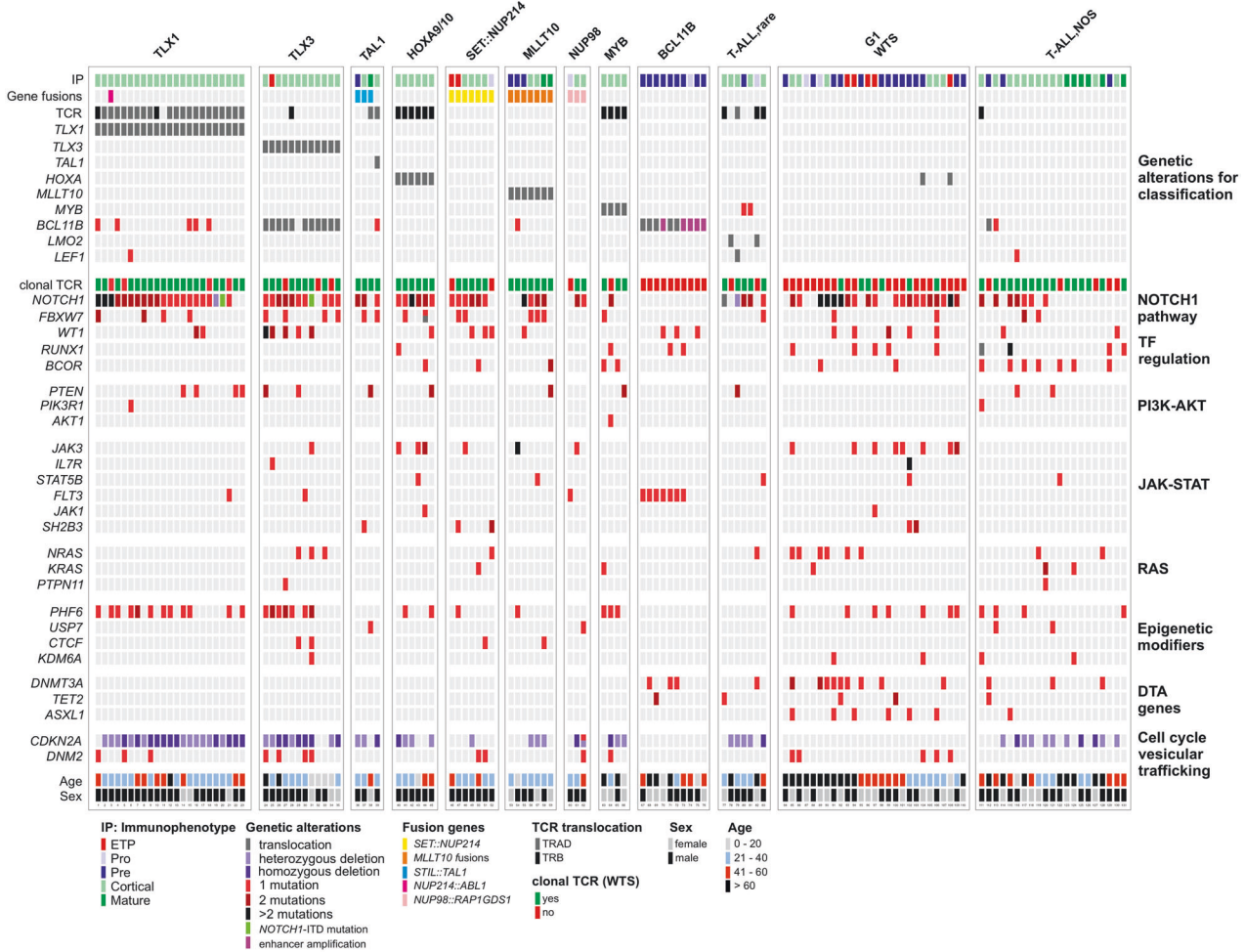


Fig. 2 Profiling of T-ALL subtypes. Immunophenotype, gene fusions, translocations, deletions, mutations, the clonality status of TCR analyzed by WTS, age and sex are depicted. Mutated genes are labeled in red (one mutation), dark red (two mutations) or black (more than two mutations). Genetic alterations in *TLX1*, *TLX3*, *TAL1*, *HOXA9/10*, *MLLT10*, *NUP98*, *MYB*, *BCL11B*, and the presence of *SET::NUP214* fusion gene allows classification into 9 distinct subgroups. Cases with rare but recurrent changes are listed as T-ALL,rare (*LMO2*-Rearrangement, *n* = 2; *TRAD::LEF1*-Rearrangement, *n* = 1; *TRB::NOTCH1*-Rearrangement, *n* = 1; *TRB::NKX2-3*-Rearrangement, *n* = 1, Mutation in *MYB* Enhancer, *n* = 2). 27 cases lacking such genetic features have a similar gene expression profile (G1). The remaining cases with no apparent common features are classified as T-ALL, NOS. Each column of the plot represents an individual case. Genetic alterations are sorted according to classification and biological pathways.

age: 32.7, 30.6, 26.4, 28.9, and 32.3 vs 43.1, and 56.2 years) (Supplementary Table 1).

In line with published data, we found that the *BCL11B* group was characterized by the absence of *NOTCH1* mutation, *PHF6* mutations and *CDKN2A* deletion, and a high frequency of *FLT3* mutations (7/10 cases, 70%, ITD: *n* = 4; TKD: *n* = 3). While cases in the *BCL11B* group showed a high expression of *KIT* and *LMO2* (Supplementary Fig. 1), we found low *RAG1* and *RAG2* expression and the absence of TCR rearrangements (Supplementary Fig. 1, Fig. 2), supporting the hypothesis that the cell of origin is a primitive hematopoietic progenitor cell, in which the ectopic

BCL11B expression induces a T-lineage transcriptional program. Cell type enrichment analyses [6] revealed that in the *BCL11B*-group granulocyte/macrophage progenitor and hematopoietic stem cells were more frequent than in the *TLX1*-, *TLX3*-, *TAL1*-group, in which dendritic cells, Th1 and Th2 cells were more frequent (Supplementary Fig. 2).

WTS has proven to be a valuable method for identification of new biological subtypes, e.g. in BCP-ALL [4, 7, 8]. Recently, a comprehensive analysis of 707 T-ALL transcriptome profiles identified 10 distinct subtypes (G1-G10) characterized by known and novel genetic aberrations and expression patterns [9].

Subgroups with high expression of *LYL1/LMO2* (G1), *GATA3* mutations (G2), *SPI1*-fusions (G3), *KMT2A*-rearrangements (G4), *MLL10*-rearrangements (G5) and *HOXA10*-fusions (G6) might represent the early T-cell progenitor, pro/precortical/cortical stage with a relatively high age of disease onset. Lymphoblasts with high expression of *TLX3* (G7) and *TLX1* (G8) could be blocked at the cortical/postcortical stage, whereas those with high expression of *NKX2-1* (G9) or *TAL1/LMO1* (G10) might correspond to cortical/postcortical/mature stages of T-cell development. We stratified our cohort into the G1-G10 expression groups (Supplementary Table 1, Supplementary Fig. 3). Subgroups G2/3/4/9 were not detectable in our cohort, as subgroups G3/4/9 are mainly present in childhood T-ALL and the G2 subgroup seems to be very rare [9]. However, the majority of our cases assigned to the NOS group belonged to the G1 group (27/48 cases, 60%). Within this G1/NOS group a subset of 21 cases did not harbor a clonal TCR rearrangement, showed low expression of *RAG1* and *RAG2* (Fig. 2, Supplementary Fig. 1), a high frequency of *DNMT3A* (7/21; 33%) and *ASXL1* mutations (4/21; 19%), no *CDKN2A* deletions and a higher median age (58 years), thus, characteristics shared with the BCL11B group. Mutations in genes involved in DNA methylation (e.g. *DNMT3A* and *TET2*) have been associated with impaired differentiation of hematopoietic stem cells [10, 11]. In our cohort, mutations in *DNMT3A*, *TET2* and *ASXL1* were exclusively detected in patients assigned to the BCL11B-, G1- or NOS group. Gene set enrichment analyses identified a strong, significant correlation of *DNMT3A* mutations with increased age (Supplementary Fig. 4). In contrast to the BCL11B group, *NOTCH1* (16/21; 76%) and *PHF6* (8/21; 38%) mutations were frequent in the G1- and NOS-groups.

Additionally, we identified seven cases with a distinct gene expression pattern characterized by high expression of *KCNKG3*, *PTPRK*, and *SCRN1* as well as low expression of *ERG*, *HOXA10*, *P2RY1*, *TTC28*, *ZBTB8A*, and *ZNF618* (Supplementary Fig. 5). All cases were classified as cortical T-ALL and harbored a clonal TCR rearrangement. In 5 cases a translocation involving *TRB* and *MYB* ($n = 3$), *RUNX1* ($n = 1$) and *NOTCH1* ($n = 1$) was observed. Interestingly, 5/7 cases harbored *BCOR* and *PHF6* co-mutations, which was observed in only two other cases in the entire cohort.

Although the cohort size is quite small we performed explorative overall survival (OS) analysis (Supplementary Fig. 6). The median survival of the total cohort was not reached with 63.4% surviving five years. The TLX1 and HOXA group demonstrated a significantly more favorable outcome, especially compared to MYB, T-ALL, NOS, or T-ALL,rare (Supplementary Table 2).

In conclusion, CBA supplemented by a FISH panel comprising six probe sets and RT-PCR screening for *STIL::TAL1*, *PICALM::MLL10*, and *SET::NUP214* allows to classify 46% of T-ALL into distinct genetically defined entities. WGS can help to further refine T-ALL classification and assign an additional 17% to distinct genetic subgroups. Due to the fact, that gene expression analysis is not a standard diagnostic technique yet we believe that a first step towards a genetic classification into a routine setting should be based on broadly available techniques. In a second step unclassified cases can be resolved by novel methods. In addition to primary genetic events used for classification, secondary events are prognostically relevant and are used for stratifying patients in clinical trials. Thus, we support a biomarker-driven classification also in T-ALL to allow subtype-associated treatment, compare responses and lead to comparability between trials as an essential step towards personalized medicine.

DATA AVAILABILITY

The datasets generated during and/or analyzed during the current study are available from the corresponding author on reasonable request.

REFERENCES

1. Khoury JD, Solary E, Abla O, Akkari Y, Alaggio R, Apperley JF, et al. The 5th edition of the World Health Organization Classification of Haematolymphoid Tumours: Myeloid and Histiocytic/Dendritic Neoplasms. *Leukemia*. 2022; 36:1703–19.
2. Alaggio R, Amador C, Anagnostopoulos I, Attygalle AD, Araujo IBO, Berti E, et al. The 5th edition of the World Health Organization Classification of Haematolymphoid Tumours: Lymphoid Neoplasms. *Leukemia*. 2022;36:1720–48.
3. Arber DA, Orazi A, Hasserjian RP, Borowitz MJ, Calvo KR, Kvasnicka HM, et al. International consensus classification of myeloid neoplasms and acute leukemia: integrating morphological, clinical, and genomic data. *Blood*. 2022; 140:1200–28.
4. Montefiori LE, Bendig S, Gu Z, Chen X, Polonen P, Ma X, et al. Enhancer hijacking drives oncogenic BCL11B expression in lineage-ambiguous stem cell leukemia. *Cancer Discov*. 2021;11:2846–67.
5. Di Giacomo D, La Starza R, Gorello P, Pellana F, Kalender Atak Z, et al. 14q32 rearrangements deregulating BCL11B mark a distinct subgroup of T-lymphoid and myeloid immature acute leukemia. *Blood*. 2021;138:773–84.
6. Aran D, Hu Z, Butte AJ. x Cell: digitally portraying the tissue cellular heterogeneity landscape. *Genome Biol*. 2017;18:220.
7. Roberts KG, Morin RD, Zhang J, Hirst M, Zhao Y, Su X, et al. Genetic alterations activating kinase and cytokine receptor signaling in high-risk acute lymphoblastic leukemia. *Cancer Cell*. 2012;22:153–66.
8. Gu Z, Churchman ML, Roberts KG, Moore I, Zhou X, Nakitandwe J, et al. PAX5-driven subtypes of B-progenitor acute lymphoblastic leukemia. *Nat Genet*. 2019;51:296–307.
9. Dai YT, Zhang F, Fang H, Li JF, Lu G, Jiang L, et al. Transcriptome-wide subtyping of pediatric and adult T cell acute lymphoblastic leukemia in an international study of 707 cases. *Proc Natl Acad Sci USA*. 2022;119:e2120787119.
10. Challen GA, Sun D, Jeong M, Luo M, Jelinek J, Berg JS, et al. Dnm3a is essential for hematopoietic stem cell differentiation. *Nat Genet*. 2011;44:23–31.
11. Izzo F, Lee SC, Poran A, Chaligne R, Gaiti F, Gross B, et al. DNA methylation disruption reshapes the hematopoietic differentiation landscape. *Nat Genet*. 2020;52:378–87.

ACKNOWLEDGEMENTS

The authors would like to thank all co-workers at the MLL Munich Leukemia Laboratory for approaching together many aspects in the field of leukemia diagnostics and research by their dedicated work, as well as all physicians for providing samples and caring for patients as well as collecting data.

AUTHOR CONTRIBUTIONS

CH and AS designed the study, JM, WW, HR, HM, IF and MLM interpreted the data, JM wrote the manuscript. JM, AS and CH were responsible for chromosome banding and FISH analyses, WW, HR, MM and HM for molecular and bioinformatic analyses, MLM and WK for immunophenotyping and TH for cytomorphologic analyses. All authors read and contributed to the final version of the manuscript.

COMPETING INTERESTS

CH, WK and TH declare part ownership of Munich Leukemia Laboratory (MLL). JM, WW, HM, IF, MLM, HR, MM and AS are employed by the MLL Munich Leukemia Laboratory.

ADDITIONAL INFORMATION

Supplementary information The online version contains supplementary material available at <https://doi.org/10.1038/s41375-022-01743-6>.

Correspondence and requests for materials should be addressed to Anna Stengel.

Reprints and permission information is available at <http://www.nature.com/reprints>

Publisher's note Springer Nature remains neutral with regard to jurisdictional claims in published maps and institutional affiliations.



Open Access This article is licensed under a Creative Commons Attribution 4.0 International License, which permits use, sharing, adaptation, distribution and reproduction in any medium or format, as long as you give appropriate credit to the original author(s) and the source, provide a link to the Creative Commons license, and indicate if changes were made. The images or other third party material in this article are included in the article's Creative Commons license, unless indicated otherwise in a credit line to the material. If material is not included in the

article's Creative Commons license and your intended use is not permitted by statutory regulation or exceeds the permitted use, you will need to obtain permission directly from the copyright holder. To view a copy of this license, visit <http://creativecommons.org/licenses/by/4.0/>.

© The Author(s) 2022, corrected publication 2022